Robust Steering Control of Spacecraft Carrier Rockets

Adriana Elysa Alimandro Correa
Alex da Rosa
Henrique Cezar Ferreira
Joao Yoshiyuki Ishihara
Renato Alves Borges
Department of Electrical Engineering
University of Brasilia
Brazil

Yuri Dmitrievich Sheptun
Physical-Technical Faculty
Dniepropetrovsk National University Oles Gonchar
Ukraine

Abstract—**In the year of 2003 it was established a cooperation agreement between Ukraine and Brazil for utilization of Cyclone-4 launch vehicle at Alcantara Launch Center. The company responsible for the marketing and operation of launch services is the company bi-national Alcantara Cyclone Space (ACS). The Cyclone-4 launch vehicle is the newest version of the Ukrainian Cyclone family launchers developed by Yuzhnoye State Design Office. This family has been used for many successful spacecrafts launches since 1969. This paper is concerned with the yaw stabilization problem around a nominal trajectory for the third stage of a satellite carrier rocket similar to the Cyclone-4. Only the steering machine of the main engine is considered as actuator. The dynamic behavior of the third stage around the nominal trajectory is modeled as a fourth-order time-varying linear system whereas the steering machine is modeled as a linear dynamical system up to third order. The values of the parameters of the steering machine model are unknown, however belonging to known intervals. As the main result, the stabilization problem is solved with a proportional derivative (PD) controller. The proposed tuning approach takes into account the robustness of the controller with respect to the steering machine model uncertainties. The performance of the PD controller is demonstrated by simulation results.**

TABLE OF CONTENTS

1. INTRODUCTION

A launch vehicle, or Rocket Carrier (RC), in general, is referred as a rocket carrying some payload into outer space [22]. There are several common characteristics which must be taken into account in designing the flight control system of a RC [22]. To achieve this objective, it is necessary to study dynamic properties of RC of spacecrafts or satellites as objects of control. This is a complex problem because the RC model is a time-variant dynamic system [5]. Rockets often require special guidance and control design strategies that are able to deal with rapidly time varying parameters [19]. With respect to the control system design, each rocket has a particular system, which depends on its structure and mission.

During the flight, the rocket is influenced by disturbance forces due to the influence of environment, the inaccuracy of rocket and propulsion manufacture and installation and the inaccuracy of elements and instruments of governance [5]. As an example, in an ideal situation, the thrust vector should be in the longitudinal axis of rocket, passing through the center of gravity. However, in practice, the thrust vector makes a small angle in relation of the longitudinal axis due to structures errors and disturbance forces. The result of this angle is three components of thrust vector, one in the longitudinal axis, as expected, and the others in the perpendicular axes to the longitudinal one, taking into account a coordinate system fixed at the center of mass in the start of launch. These cause a small variation in the angles of pitch and yaw and a center of mass displacement. To circumvent this problem of stability, it used, in the present work, a thrust vector control system actuating in a single engine rocket. The vector control is applied in space vehicle nozzles to change the thrust direction in order to perform maneuvers and small deviations [21]. An electro-hydraulic servo valve, thereafter called steering machine (SM), is used as actuator.

The electro-hydraulic servo valves have been studied for many years [1, 6–8, 10–12, 15]. In [1], for example, it is showed that until 1957, there was around 21 different servo valve designs. These are used in industrial applications, such as testing equipments and autonomous manufacturing systems [15], in flight simulations and robots [7], and, in the aerospace industry, for flight attitude control of rockets [11]. Nowadays, in all spacecraft, it is common to use hydraulic actuators to vary the engine angle [8]. A lot of studies about these valves are found in the literature, such as discussion on some issues involved in controlling linear hydraulic actuators [6], modeling and control of a hydraulic servo system [7] and designing of a proportional integral derivative controller attached to electro-hydraulic servo actuator system [10]. Control of the angular position of the rotary actuator, which controls the movable surface of space vehicles is also studied in [10]. A mathematical model for an electro-hydraulic servo directional valve is presented in [12] and a comprehensive dynamic model of a closed-loop servo-valve controlled hydro-motor drive system is proposed in [15].

Some investigations about nozzle vector control have been applied to a mini-launcher [17]. The principles of analysis and design of launch vehicle flight control are described in [9], where stability robustness with respect to modeling

978-1-4577-0557-1/12/$26.00 ©2013 IEEE.
[1] IEEEAC Paper #xxxx, Version x, Updated dd/mm/yyyy.

uncertainties and a gimbal angle constraint is discussed. In [20] a thrust vector control of an upper-stage rocket with multiple propellant slosh modes is proposed, where the control inputs are defined by the gimbal deflection angle of a main engine and a pitching moment about the spacecraft center of mass. The electro-hydraulic thrust vector control of twin rocket engines with position feedback was presented [8], and a comparison between mechanical and gas-dynamic control system of space vehicle is discussed [18]. In [18], a mathematical model using mechanical control system that describes the angular motion of a closed loop dynamic system in the plane of yaw is considered.

In the present work, a third stage rocket stability control problem using a SM as actuator of a single engine is investigated. As an example, it is used a rocket similar to Cyclone-4, which is the newest version of the Ukrainian Cyclone family launchers developed by Yuzhnoye State Design Office. This family has been used for many successful spacecrafts launches since 1969. To solve the rocket stability control problem, the proposed approach involves:

1. to obtain the equations that describe the system,
2. to calculate the coefficients that vary in time,
3. to construct stability areas,
4. to select the structure and parameters of control system,
5. to validate the choices by mathematical modeling of movement.

The remainder of this paper is organized as follows. Section 2 presents a description of the control problem, Section 3 describes the electro-hydraulic servo valve model. Section 4 presents the description of dynamic system non-stationary mathematical model and calculation of equations parameters. Section 5 is about the construction of stability areas. Section 6 shows the results of control problem to stabilize the yaw angle by designing a PD controller. Finally, Section 7 presents the conclusions.

2. DESCRIPTION OF THE PROBLEM

Consider the following coordinate systems:

• a coordinate system fixed on the Earth - $X_0Y_0Z_0$, in the initial position of rocket at launch site, as shown in Figure 1;
• a coordinate system fixed in the center of mass (CM) of rocket - XYZ, where X coincides with the direction of the velocity vector and tangent of rocket trajectory, as shown in Figure 2;
• a coordinate system related to the rocket, fixed at the initial position of CM in the start of launch - $X_1Y_1Z_1$, where X_1 is aligned with the rocket longitudinal axis and Y_1 is located in the plane of symmetry of rocket, as shown in Figure 2;

In Figure 1, the angle in the plane X_0Y_0 between the horizon line and X_1 is the angle of pitch ϕ and the angle in the plane X_0Z_0 between X_1 and the plane X_0Y_0 is the yaw angle ψ (figure 2). The initial coordinate system is used to determine the position of the rocket as a rigid body in space [5].

In Figure 2, I, II, III and IV represent the symmetrical axis of rocket and V is the velocity of the rocket. The plane I-III coincides with the plane of fire X_0Y_0, and Y_0 is positive direction taken from the Earth's surface [5].

In an ideal situation, the rocket thrust vector should be in the longitudinal axis of rocket, passing through the center of gravity, resulting in a maximum impulse. But, in practice,

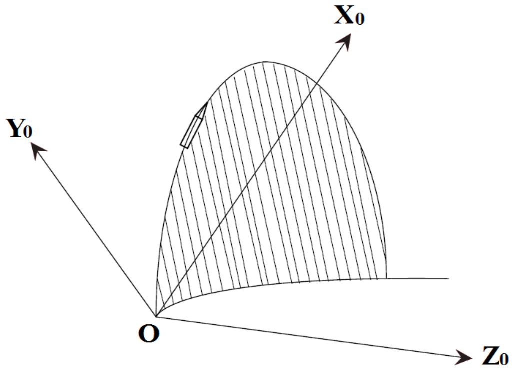

Figure 1. Initial coordinate system $X_0Y_0Z_0$

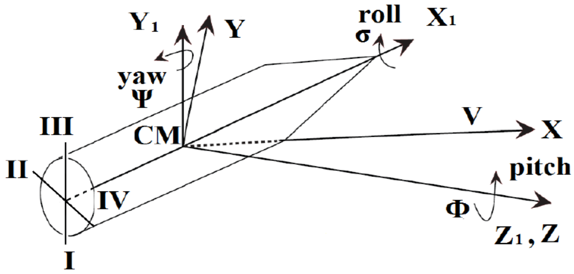

Figure 2. Coordinate system related to the rocket $X_1Y_1Z_1$ and coordinate system XYZ situated in the center of mass of the rocket

the mass distribution, small structure errors and disturbance forces result in a small angle of thrust vector with respect to this longitudinal axis X_1. This angle, in turn, results in three components of thrust vector: one in the axis X_1, one toward to the lateral in the direction of Z_1 (yaw plane) and one in direction of Y_1 (pitch plane). The lateral component on the yaw plane is responsible for a moment that results in an initial small angle of yaw and a CM lateral displacement with respect to the longitudinal axis, causing instability of the rocket. There are some different ways to deal with this instability. For example, for the third stage control system of a rocket similar of Cyclone-4 with a single engine, it is possible to vary the engine angle within a small range (usually less than 1^o) for the upper stages [4]. In this problem it is considered an angle not greater than 5^o, generating a moment about the center of mass and maintaining the rocket stable in a previous established nominal trajectory area. This scheme is depicted in Figure 3, where P is the thrust vector and δ is the gimballed angle.

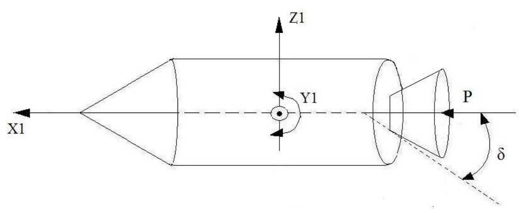

Figure 3. Scheme of rocket gimbaled engine

To control the thrust vector, an SM can be used. This device turns an electrical current into a hydraulic flow that can generate a mechanical motion; linear, rotational, shuttle or unidirectional [13]. It is possible to model an electro-hydraulic servo valve at various levels of detail, depending on the project application. For example, when designing the valve, more detail is needed than when modeling a system controlled by an already designed one [2]. Its dynamic can generally be described by first and second-order transfer functions [15]. The servo-valve mechanism can be variable in its weight, size, capacity and efficiency. The characteristics of an SM depends on the rocket and engine structure, as well as on the mission to be developed. To increase the payload and decrease the rocket mass, it is better if the SM is small and has a high capacity, generating a fast response of the engine. To understand better the dynamic of the electro-hydraulic servo valve, a third stage rocket mathematical model and stability study are presented.

3. Electro-hydraulic servo valve: an example

Consider an SM composed by an eletric RL circuit connected to a steel rod that can move to the left or to the right by an Small angle θ. The rod is kept from each of two nozzles by twice the distance and is very small, with weight less than 0.005kg. Connected to each nozzle is a valve that attaches them to a hydraulic actuator. One of the nozzles is coupled to a piston system. The actuator works with the difference of pressure between one of the nozzles (P_4) and the piston system (P_3). The system of SM is shown in details in Figure 4, enlarged in relation to the rocket engine.

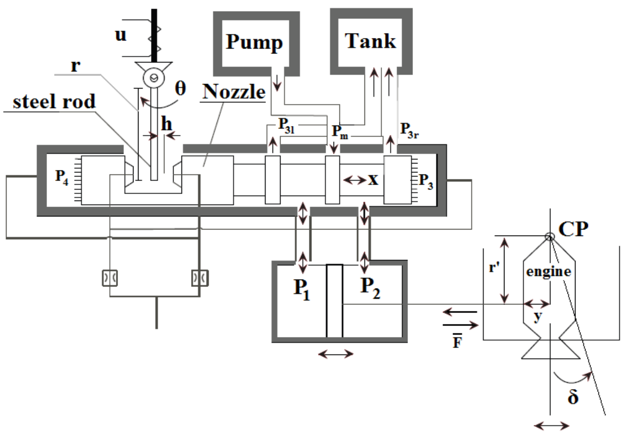

Figure 4. Sketch of the interaction of SM with a rocket managing engine

When pressure P_3 is equal to pressure P_4, the system is in equilibrium and the rod is exactly at the middle of distance between the two nozzles. In other words, the valve is in the null position. Moving the rod to the right until h by an electric impulse with an applied tension u, P_4 becomes greater than P_3 and the system composed by nozzles and pistons moves to the right, opening a gap to the pipes. The pump leads special oil (working liquid) from P_m to P_1 and, as result, $P_1 > P_2$. After that, the oil from P_2 goes to tank passing through P_{3r} and the piston between P_1 and P_2 moves to the right in a distance y. The thrust vector direction changes and the angle δ that rocket makes with its longitudinal axis becomes nonnull.

Thereafter, the closed-loop system receives a negative feedback until the input is equal to zero and the rod is exactly in the middle of distance between the two nozzles again. Thus the system composed by nozzles and pistons returns to the initial position. The rod is moved to the left by other electric impulse, $P_4 < P_3$, the system also moves to the left, and the pump leads working liquid from P_m to P_2 until $P_1 = P_2$. In this situation, one has $P_1 = P_2$ and $\delta = 0$. Again, by feedback, the input becomes equal to zero, and the system is at the null position. A similar procedure occurs when the system is in equilibrium and the rod moves first to the left.

Summarizing, three cases can be considered:

1. $u = 0$ and $\delta = 0$: valve at the null position ($P_3 = P_4$);
2. $u > 0$ and $\delta \neq 0$: after the rod has been moved;
3. $u = 0$ and $\delta \neq 0$: after feedback.

The system that represents the SM and the actuation on the engine is shown in Figure 5.

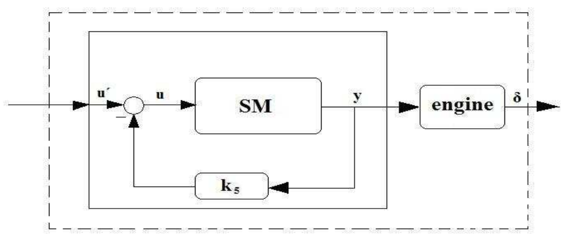

Figure 5. Representation of electro-hydraulic servo valve and its actuation at engine

To the open loop system, the electric RL circuit may be described by the following differential equation [3]:

$$T_1 \frac{dI}{dt} + I = k_1 u, \qquad (1)$$

where $T_1 = \frac{L}{R}$, $K_1 = \frac{1}{R}$, L is the inductance and R the resistance.

The electrical current I moves the steel rod, so it is the input to other control block whose output is h, the steel rod block. The equation that describes this block is a second-order differential equation given by

$$m_1 \frac{d^2 h}{dt^2} + b_1 \frac{dh}{dt} + C_1 h = k_2 I, \qquad (2)$$

where the constants b_1, C_1 and k_2 are obtained experimentally, k_2 is a constant of proportionality, b_1 is related with the expenses of viscous friction energy and the moment of Coriolis force due to stream of nozzles gas, and C_1 is related with the damped motion of steel rod. The first term in (2) is obtained from the steel rod moment equation.

Figure 4 shows a steel rod described as a very small rod near the eletric circuit, in which the moment is represented by $I\ddot{\theta} = M$, where I is the moment of inertia and θ the angle of rod rotation. From this figure, it is possible to write $h = r\theta$ for small θ values. By deriving this equation twice and substituting in the moment equation $\ddot{\theta} = \ddot{h}/r$, it yields $M = \ddot{h}I/r$. So, the moment of inertia can be written as $I/r = m_1$. Thus, $\ddot{h}m_1 = M$.

It is possible to rewrite equation (2) as follows [3]:

$$T_2^2 \frac{d^2h}{dt^2} + 2\zeta_2 T_2 \frac{dh}{dt} + h = K_2 I, \tag{3}$$

where $T_2^2 = \frac{m_1}{C_1}$, $2\zeta_2 T_2 = \frac{b_1}{C_1}$ and $K_2 = \frac{k_2}{C_1}$.

The output h becomes input to the variation of the piston system. Being A_3 the section area of piston system and k_3 a constant of proportionality, it is possible to write [3]:

$$T_3 \frac{dx}{dt} + x = h, \tag{4}$$

where $T_3 = A_3/k_3$.

Position x is the input to the variation of pressure $\Delta P = P_1 - P_2 = k_4 x$, and ΔP is the input to the displacement y of the piston between P_1 and P_2. The equation that describes the displacement piston control blocks is:

$$m_4 \frac{d^2y}{dt^2} + b_4 \frac{dy}{dt} + C_4 y = A_4 k_4 x, \tag{5}$$

where b_4 is related with the expenses of viscous friction energy and the moment of Coriolis force due to stream of engine gas, C_4 is related with the moment of engine displacement, and k_4 is a constant of proportionality. The first term of equation (5) can be described as moment of engine movement.

Figure 4 shows an example of engine movement, where δ is the engine angle, $\bar{F}$ is the force applied by movement of piston in the engine, and r' is the distance between the center of pressure (CP) and the engine point where the force $\bar{F}$ is applyed. CP is the point of rocket where all the fluid pressure forces are concentrated (in this case the thrust vector). $\bar{F}$ is applied to the CM. Since $y = r'\delta$ and the moment equation is given by $I_g\ddot{\delta} = M$, then for $\ddot{y} = r'\ddot{\delta}$, it is possible to write $I_g\ddot{y}/r' = M$, where $I_g/r' = m_4$, and $m_4\ddot{y} = M$. It is important to remark that this last equation does not take into account compressibility of liquid, nonlinear dependences, and so on. The equation (5) also can be rewritten as:

$$T_4^2 \frac{d^2y}{dt^2} + 2\zeta_4 T_4 \frac{dy}{dt} + y = \frac{A_4 k_4}{C_4} x, \tag{6}$$

where $T_4^2 = \frac{m_4}{C_4}$ and $2\zeta_4 T_4 = \frac{b_4}{C_4}$.

Finally, considering $r' = 1$m, one has $|y| = |\delta|$. The block diagram of the open loop SM is shown in Figure 6.

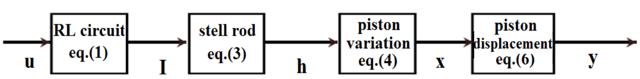

Figure 6. Block diagram of the SM in open loop

In order to study this isolated system and its stability, the open and the closed loop are considered. For the closed loop, the equations are almost the same ones than those of the open loop, however replacing u by the feedback control $u' - k_5 y$, where k_5 is a system proportional gain:

$$T_1 \frac{dI}{dt} + I = k_1(u' - k_5 y). \tag{7}$$

It is clear that the SM is described by a set of differential equations formed by (1), (3), (4), (6). To solve them, first of all, the variation of parameters with respect to time is studied. As $|y| = |\delta|$, the calculations were performed using only y.

Open loop and closed loop systems

Open loop—The parameters used in the computational simulations are shown in Table 1 [3].

Table 1. Parameters of the SM

Parameter	Value
T_1	$0.01s$
k_1	$0.005\Omega^{-1}$
b_1	$3.5kg/s$
C_1	$12500N/m$
m_1	$4500kg$
u	$20V$
k_2	$12.5N/A$
T_3	$100s$
m_4	$1kg$
b_4	$20kg/s$
C_4	$10^4N/m$
A_4	10^4m^2
k_4	$2000V/m$

By denoting $Q_{ol}(0)$ the matrix containing the initial values of parameters I, h, $\dot{h}$, x, y, and $D_{ol}(t,x)$ the matrix representing the set of differential equations for the open loop system, one has:

$$\begin{aligned} Q_{ol}(0) &= \begin{bmatrix} I_0 & h_0 & \dot{h}_0 & x_0 & y_0 & \dot{y}_0 \end{bmatrix}^T \\ &= \begin{bmatrix} 0 & 0 & 0 & 0 & 0 & 0 \end{bmatrix}^T . \end{aligned}$$

Equations (1), (3), (4) and (6) can be rewritten as follows:

$$D_{ol}(t,x) = \begin{pmatrix} \frac{k_1 u - I}{T_1} \\ \dot{h} \\ \frac{k_3 I - 2T_2\zeta_2\dot{h} - h}{T_2^2} \\ \frac{h - x}{T_3} \\ \dot{y} \\ \frac{\frac{A_4 k_4 x}{C_4} - 2T_4\zeta_4\dot{y} - y}{T_4^2} \end{pmatrix},$$

where $\zeta_2 = \frac{b_1}{2\sqrt{C_1 m_1}}$ and $k_3 = \frac{k_2}{C_1}$. The graphics obtained applying the step u with amplitude of $20V$ are shown in Figure 7.

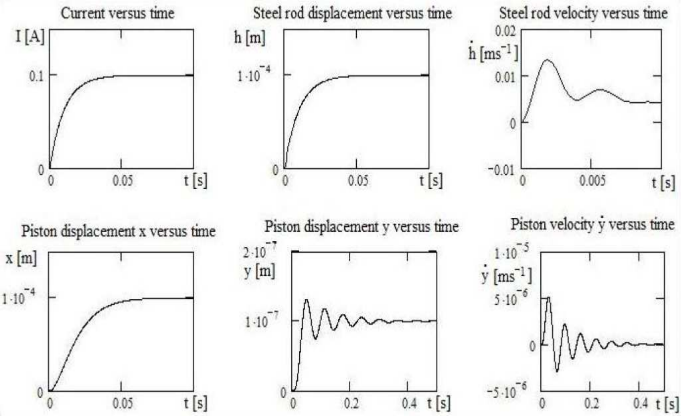

Figure 7. Open loop graphics of variation of parameters with time

Closed loop—For the closed loop system, it is used a step U with amplitude of $U = u' - k_5 y$, where $k_5 = 2 \cdot 10^3$ and $u' = 20V$. The initial values of parameters and the set of differential equations are given by:

$$\begin{aligned} Q_{cl}(0) &= \begin{bmatrix} I_0 & h_0 & \dot{h}_0 & x_0 & y_0 & \dot{y}_0 \end{bmatrix}^T \\ &= \begin{bmatrix} 0 & 0 & 0 & 0 & 0.01 & 0 \end{bmatrix}^T, \end{aligned}$$

$$D_{cl}(t,x) = \begin{pmatrix} \frac{k_1(u' - k_5 y) - I}{T_1} \\ \dot{h} \\ \frac{k_3 I - 2T_2\zeta_2\dot{h} - h}{T_2^2} \\ \frac{h - x}{T_3} \\ \dot{y} \\ \frac{\frac{A_4 k_4 x}{C_4} - 2T_4\zeta_4\dot{y} - y}{T_4^2} \end{pmatrix}.$$

The graphics for the closed loop are shown in Figure 8.

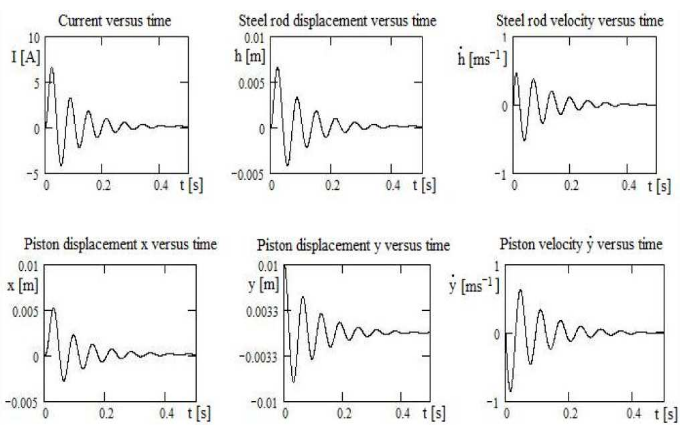

Figure 8. Closed loop graphics of variation of parameters with time

Analyzing these graphics in Figs. 7 and 8, one can see that the state variables converge to a single point and none of them goes to infinity, so the system is stable. Studying the blocks of piston variation and piston displacement of device with and without damping, it was seen that the systems with damping converge faster than the systems without damping.

To calculate the roots of the characteristic equation of the open loop and closed loop systems, it is necessary to rewrite the differential equations in the Laplace domain:

Open loop—

$$\begin{cases} (T_1 s + 1)I(s) = k_1 U(s), \\ -k_2 I(s) + (m_1 s^2 + b_1 s + C_1)H(s) = 0, \\ -H(s) + (T_3 s + 1)X(s) = 0, \\ -\frac{A_4 K_4}{C_4}X(s) + (T_4^2 s^2 + 2\zeta_4 T_4 s + 1)Y(s) = 0. \end{cases} \tag{8}$$

The roots of the open loop system are computed as:

$$Z_{ol} = \begin{pmatrix} -388.889 + 1621i \\ -388.889 - 1621i \\ -100.014 - 0.027i \\ -99.986 + 0.027i \\ -10 + 99.499i \\ -10 - 99.499i \end{pmatrix}.$$

Closed loop—

$$\begin{cases} (T_1 s + 1)I(s) + k_1 k_5 s Y(s) = k_1 U'(s), \\ -k_2 I(s) + (m_1 s^2 + b_1 s + C_1)H(s) = 0, \\ -H(s) + (T_3 s + 1)X(s) = 0, \\ -\frac{A_4 K_4}{C_4}X(s) + (T_4^2 s^2 + 2\zeta_4 T_4 s + 1)Y(s) = 0. \end{cases} \tag{9}$$

The roots of the closed loop system are computed as:

$$Z_{cl} = \begin{pmatrix} -388.889 - 1621i \\ -388.889 + 1621i \\ -102.387 \\ -97.615 \\ -9.999 - 99.527i \\ -9.999 + 99.527i \end{pmatrix}.$$

By analyzing the roots of the open and closed loop system, it is also possible to see that its real part is negative, so the system is stable.

A more general equation

As said before, it is possible to model an electro-hydraulic servo valve at various level of detail depending of the objective. Consider again the system of differential equation (8) of the SM. By isolating I in the first equation of this system of equations, one has:

$$I = \frac{K_1}{(T_1 s + 1)} u.$$

Replacing I in the second equation and isolating h:

$$h = \frac{K_1 K_2}{(T_1 s + 1)(T_2^2 s^2 + 2\zeta_2 T_2 s + 1)} u.$$

Again replacing h in the third equation and isolating x:

$$x = \frac{K_1 K_2}{(T_1 s + 1)(T_2^2 s^2 + 2\zeta_2 T_2 s + 1)(T_3 s + 1)} u.$$

Finally, replacing x in the last equation:

$$y = \frac{A_4 K_4 K_1 K_2 u}{\eta},$$

where $\eta = (T_1 s + 1)(T_2^2 s^2 + 2\zeta_2 T_2 s + 1)(T_3 s + 1)(T_4^2 s^2 + 2\zeta_4 T_4 s + 1)$.

Using $|y| = |\delta|$, one gets the following 6th-order transfer function:

$$\eta y = A_4 K_4 K_1 K_2 u. \tag{10}$$

Since the steel rod is considered very small and moves along with a small distance or angle, such as the piston system, in general T_1, T_2 and T_3 are small. Because of that, equation (10) can be approximated by a 3rd-order transfer function:

$$(\tau_1 s + 1)(\tau_2^2 s^2 + 2\zeta\tau_2 s + 1)\delta = u_c, \tag{11}$$

where ζ is a damping factor, τ_1 and τ_2 are time constants, δ the angle of engine movement (output), u_c the input. The damping factor ζ is determined by the frictional forces in the bearings of mobile connections and may vary slightly. The values of τ_1 and τ_2 are determined by mass and geometry (size) of governing bodies, in particular the control engines. They are defined as induced drag, present in the control devices.

4. Non-stationary mathematical model of dynamic system and calculation of parameters

Using a thrust vector control system, it is possible to gimbal the engine in order to maintain the rocket stability in a previous established nominal trajectory area. For this, it is necessary to obtain the equations that describe the dynamic of rocket third stage. Those equations describe the lateral CM displacement acceleration and the acceleration of yaw angle. In this problem only the control of yaw in its plane is considered, supposing that the control of pitch and yaw are independent because of the approximation of small angles ($\delta \leq 5^{\circ}$). The equations in the pitch plane are very similar to the equations of yaw in this case.

The equation of CM lateral displacement acceleration is directly proportional to CM lateral displacement velocity, yaw angle, variation of yaw, the SM angle and the resultant force of disturbance:

$$\begin{aligned} \ddot{z} &= a_{zz}\dot{z} + a'_{z\psi}\dot{\psi} + a_{z\psi}\psi + a_{z\delta}\delta + \bar{F}_z, \\ \bar{F}_z &= \frac{F_z}{m}, \end{aligned} \tag{12}$$

where z is the rocket lateral deviation of the CM, m is the third stage mass and F_z the perturbed resultant force [5]. This resulting disturbance force can be caused by action of wind (not in this case because it is considered the mathematical model of third stage), presence of manufacturing and assembly (installation) errors of a rocket and driving force installation.

Due to skew and frame deformation respectively, two perturbed forces are considered in the model: $F_1 \approx P\sin(\frac{5}{60}^{\circ})$ and $F_2 \approx P\sin(\frac{10}{60}^{\circ})$. The force F_z is calculated as $F_z = \sqrt{F_1^2 + F_2^2}$ [16], see Figure 9.

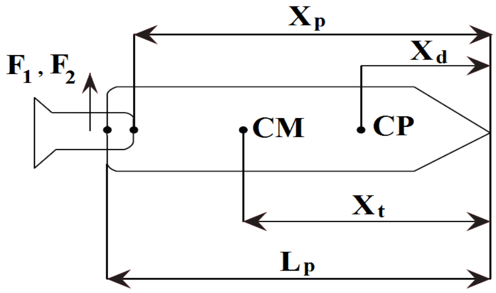

Figure 9. Perturbed forces due to skew and frame deformation

The time-variant parameters a_{zz}, $a_{z\psi}$, $a'_{z\psi}$ and $a_{z\delta}$ can be calculated using experimental values [16] of thrust, mass, dimensions of rocket, forces, density of air and area of transversal section. This model does not consider the terms that depends of flow rate of total mass and the flow of mth tank. In the third stage, the density of air (ρ) is considered negligible and the parameters a_{zz} and $a'_{z\psi}$ can be considered zero [5], since these are dependent on the air density.

The equation for the acceleration of yaw angle is similar to the equation of CM lateral displacement acceleration, but it is dependent of resultant moment of disturbance:

$$\begin{aligned} \ddot{\psi} &= a_{\psi z}\dot{z} + a'_{\psi\psi}\dot{\psi} + a_{\psi\psi}\psi + a_{\psi\delta}\delta + \bar{M}_z, \\ \bar{M}_z &= \frac{M_z}{I_g}, \end{aligned} \tag{13}$$

where I_g is the inertial moment of stage and M_z the resultant of perturbed moment. Once again, the parameters can be calculated using data from [16] and as $\rho = 0$, the parameters $a_{\psi z}$, $a'_{\psi\psi}$ and $a_{\psi\psi}$, which depend on ρ, will be considered zero [5].

Due to skew and frame deformation forces, F_1 and F_2, the arising moments are $M_1 = F_1(L_p - X_t)$ and $M_2 = F_2(L_p - X_t)$ (see Figure 9), which result in $M' = \sqrt{M_1^2 + M_2^2}$. Also, moments of disturbance arise due to displacement of the CM. In the yaw plane, the moment M_z^* is calculate as $M_z^* = P z_T^H$, where z_T^H is the distance component of CM in the axis z_1 (see Figure 10). The resultant of perturbed moment, M_z, is calculated as $M_z = M' + M_z^*$. y_T^H is the distance component of CM in the axis y_1.

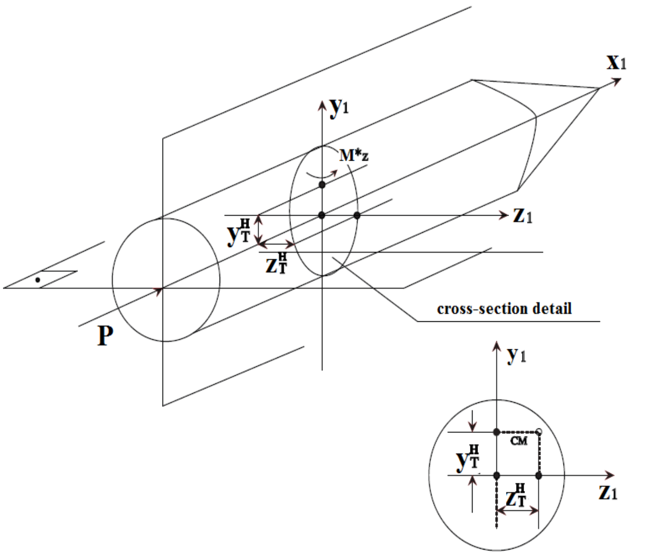

Figure 10. Moment of disturbance relative to CM displacement

To simplify this complex problem, a PD controller actuating only on the angle of yaw is considered. For this, one has the law control $u_c = K_p\psi + K_d s\psi$, where K_p and K_d are the constants to be determinate (controller gains). Finally, the set of equations for a rigid hardened rocket that describes the stability problem is as follows:

$$\begin{cases} s^2 z - a_{z\psi}\psi - a_{z\delta}\delta = \bar{F}_z, \\ s^2\psi - a_{\psi\delta}\delta = \bar{M}_z, \\ (\tau_1 s + 1)(\tau_2^2 s^2 + 2\zeta\tau_2 s + 1)\delta = u_c, \\ u_c = K_p\psi + K_d s\psi. \end{cases} \tag{14}$$

The used data are close to those of the Cyclone-4 third stage [16] whitin the time interval from 0 through 0.7s. Aerodynamic factors are considered negligible since the air density is disregarded.

The factor $a_{z\delta}$ is calculated as $a_{z\delta} = -P_0/m$, where P_0 is the thrust engine in Earth and m is the mass of the rocket at the third stage, calculated as $m = G(t)/9.81$. $G(t) = G_0 - G'$ is the variation in weight with time, where G_0 is the initial values of weight and G' the change in weight with time.

To calculate $a_{\psi\delta}$, it is necessary to use the values of thrust engine on Earth, the coordinate P_0 of CM; X_t; the coordinate of engine location, $X_p = L_p - 1$; and the inertia moment obtained from $a_{\psi\delta} = -P_0(X_p - X_t)/I$. L_p is the distance between the beginning of third stage rocket and the end, not considering the engine. Figure 9 shows a sketch of distances X_t, X_p, L_p and X_d distance of CP to the top of rocket.

Factor $a_{z\psi}$ is obtained as $a_{z\psi} = -P/m$, where P is the thrust engine by approximating to small angles, $P\cos(\alpha) = P$ and $P\sin\alpha = P\alpha$. At least, $\bar{F}_z = F_z/m$ is also calculated as already explained. All the factors were computed in the yaw plane.

During the time interval 0 through 0.25s, all the parameters are null, so the polynomial regression can be performed considering only the interval $[0.3, 0.7]$s. A fourth-order polynomial has been used to iterpolate the data. Figure 11 shows the graphics obtained comparing the used time-variant data [16] to the polynomial regression for each one of parameters.

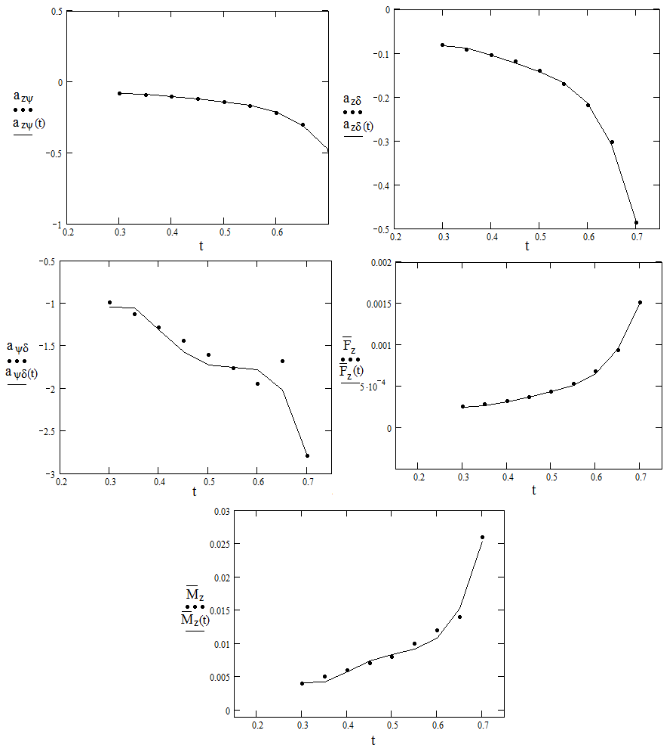

Figure 11. Graphics of the polynomial regression

Finally, the mathematical modeling of the time-variant system has been obtained. The polynomial functions obtained for each one of parameters are given as follows:

$$\begin{aligned} a_{z\psi} \quad (t) &= -2.047 + 19.027t - 67.266t^2 + 103.296t^3 - 59.254t^4, \\ a_{z\delta} \quad (t) &= -2.047 + 19.027t - 67.266t^2 + 103.296t^3 - 59.254t^4, \\ a_{\psi\delta} \quad (t) &= -33.285 + 299.319t - 1003t^2 + 1437t^3 - 751.562t^4, \\ \bar{F}_z \quad (t) &= 6.679 \cdot 10^{-3} - 0.062t + 0.218t^2 - 0.333t^3 + 0.19t^4, \\ \bar{M}_z \quad (t) &= 0.216 - 2.009t + 6.912t^2 - 10.246t^3 + 5.594t^4. \end{aligned} \tag{15}$$

The set of equations is given by:

$$\begin{cases} s^2 z - a_{z\psi}\psi - a_{z\delta}\delta = \bar{F}_z, \\ s^2\psi - a_{\psi\delta}\delta = \bar{M}_z, \\ -(K_p + K_d s)\psi + [\tau_1\tau_2^2 s^3 + (2\zeta\tau_1\tau_2 \\ +\tau_2^2)s^2 + (\tau_1 + 2\zeta\tau_2)s + 1]\delta = 0, \end{cases} \tag{16}$$

or, in the time domain:

$$\begin{cases} \frac{d^2 z}{dt^2} = a_{z\psi}(t)\psi + a_{z\delta}(t)\delta + \bar{F}_z(t), \\ \frac{d^2\psi}{dt^2} = a_{\psi\delta}(t)\delta + \bar{M}_z(t), \\ -(K_p\psi + K_d\frac{d\psi}{dt}) + \tau_1\tau_2^2\frac{d^3\delta}{dt^3} \\ +(2\zeta\tau_1\tau_2 + \tau_2^2)\frac{d^2\delta}{dt^2} + \\ (\tau_1 + 2\zeta\tau_2)\frac{d\delta}{dt} + \delta = 0. \end{cases} \tag{17}$$

5. STUDY OF STABILITY AREAS

In order to evaluate the control stability problem, first consider the analysis of area stability construction. To deliver the payload to a given point on the space, it is considered a region around the nominal trajectory, i.e., a technical stability region. That means that if the rocket is maintained inside this region, the mission would be accomplished. Taking different instants of time ($t = 0.3s, t = 0.4s, t = 0.5s, t = 0.6s, t = 0.7s$) and setting the parameters values at these instants [16], areas of stability are constructed for some probable values of constants τ_1 and τ_2 in order to analyze the influence of these constants on the size of stability areas. For each instant of time there are different coefficient values of movement equations of rocket and different stability areas.

The study of the influence of τ_1 and τ_2 on the size of the areas is important for solving the control problem. These values are generated for design parameters and cannot be chosen arbitrarily. They may vary slightly and, in the design, they can be changed within some range. It is considered the variation of τ_1 and τ_2 between 0.001 and 0.15. Each point inside the stability region defines the coordinates τ_1, τ_2, K_p and K_d, indicating the values of time constants and gains in the implementation that provide the stable movement of rocket. The time constants are chosen before constructing the areas, such as the SM damping factor, chosen between 0.1 and 0.4 (in most of stability area construction was used $\zeta = 0.3$). The limits of stability regions moves in τ_1, τ_2, K_p, K_d because of changes in movement equation coefficients. It is possible that the selection of the values in the initial instant of design is not inside the stability region in some moment of flight. In this case, τ_1 and τ_2 cannot change, so it is necessary to change the value of length r' in the SM, the shoulder of control force relative of CM. The calculation of boundary stability enables the choice of gain value, formed by the control system and implemented as needed.

First, it is chosen a time instant to set the parameters $a_{z\psi}(t)$, $a_{z\delta}(t)$ and $a_{\psi\delta}(t)$ is chosen. Then, one isolates δ in the third equation of 16 and replaces in the first two system equations. Finally, the resulting equations are written in the matrix form:

$$\begin{bmatrix} s^2 & (-a_{z\psi}) - \frac{(a_{z\delta}K_p + a_{z\delta}K_d s)}{(\tau_1 s+1)(\tau_2^2 s^2 + 2\zeta\tau_2 s+1)} \\ 0 & (s^2 - \frac{(-a_{\psi\delta}K_p + a_{\psi\delta}K_d s)}{(\tau_1 s+1)(\tau_2^2 s^2+2\zeta\tau_2 s+1))} \end{bmatrix} \begin{bmatrix} z(s) \\ \psi(s) \end{bmatrix}$$

$$= \begin{bmatrix} \bar{F}_z(s) \\ \bar{M}_z(s) \end{bmatrix}. \tag{18}$$

The characteristic polynomial of the first matrix of above equation, calculated at $s = jw$, can be written as:

$$A_{11}(w)K_p + A_{12}(w)K_d = B_1(w),$$

$$A_{21}(w)K_p + A_{22}(w)K_d = B_2(w).$$

Then, by defining:

$$\Delta(w) = \begin{vmatrix} A_{11}(w) & A_{12}(w) \\ A_{21}(w) & A_{22}(w) \end{vmatrix},$$

$$\Delta_1(w) = \begin{vmatrix} -B_1(w) & A_{12}(w) \\ -B_2(w) & A_{22}(w) \end{vmatrix},$$

$$\Delta_2(w) = \begin{vmatrix} A_{11}(w) & -B_1(w) \\ A_{21}(w) & -B_2(w) \end{vmatrix},$$

one finally gets the PD controller parameters:

$$K_p(w) = \frac{\Delta_1(w)}{\Delta(w)}, \quad K_d(w) = \frac{\Delta_2(w)}{\Delta(w)}. \tag{19}$$

For instance, at $t = 0.3s$ the polynomials $a_{z\psi}(t), a_{z\delta}(t), a_{\psi\delta}(t)$ are evaluated as:

$$a_{z\psi}(0.3) = -0.084,$$
$$a_{z\delta}(0.3) = -0.084,$$
$$a_{\psi\delta}(0.3) = -1.048.$$

In this example, the range of frequency for the calculation of K_p, K_d is $w \in [0, 100]$ rad/s and the damping factor is $\zeta = 0.3$. By varying the time constants, the stability areas can be constructed. As an example, considering the variation of τ_2 inside the interval $[0.1, 0.15]$ with fixed $\tau_1 = 0.01s$, one obtains the plot shown in Figure 12. Similarly, for fixed $\tau_2 = 0.01s$ and varying τ_1 inside the interval $[0.1, 0.15]$, one obtains the plot shown in Figure 13.

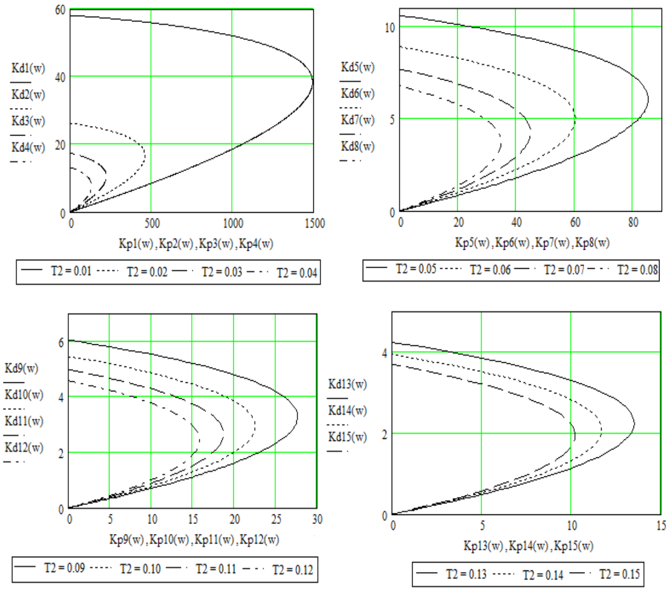

Figure 12. Areas of stability - τ_1 fixed

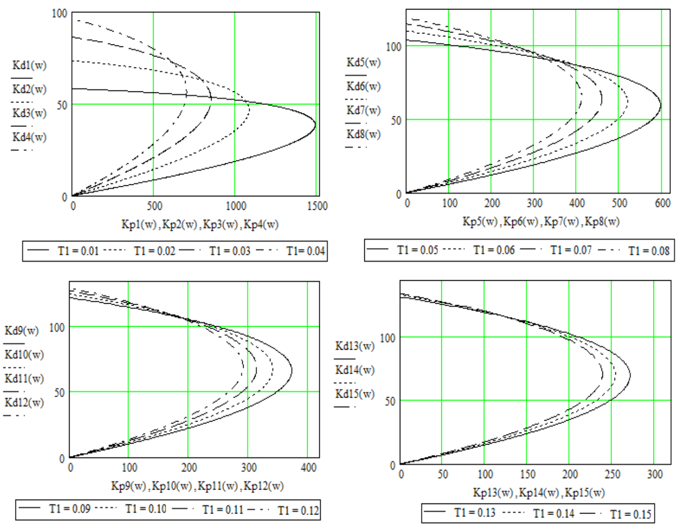

Figure 13. Areas of stability - τ_2 fixed

It can be observed that the stability areas in Figure 12 decrease as τ_2 increases. In Figure 13, the stability areas decrease less than in Figure 12, but these areas are a little dislocated as τ_1 increases.

6. Development and Results

Consider again the mathematical model of the time-variant system. Another approach studied in this work is to choose $\tau_{1\,\min} \leq \tau_1 \leq \tau_{1\,\max}$, $\tau_{2\,\min} \leq \tau_2 \leq \tau_{2\,\max}$, K_p and K_d in such a way that the yaw angle and its variation to be stable (converging to zero). The parameters $a_{z\psi}, a_{z\delta}$ and $a_{\psi\delta}$ are considered fixed at a given time instant.

Define the following state-space variables:

$$\begin{aligned} z &= x_0, \\ \frac{dz}{dt} &= \frac{dx_0}{dt} = x_1, \\ \psi &= x_2, \\ \frac{d\psi}{dt} &= \frac{dx_2}{dt} = x_3, \\ \delta &= x_4, \\ \frac{d\delta}{dt} &= \frac{dx_4}{dt} = x_5, \\ \frac{d^2\delta}{dt^2} &= \frac{dx_5}{dt} = x_6. \end{aligned} \tag{20}$$

The set of equations (17) is written as:

$$\begin{cases} \frac{dx_0}{dt} = x_1, \\ \frac{dx_1}{dt} = a_{z\psi}(t)x_2 + a_{z\delta}(t)x_4 + \bar{F}_z, \\ \frac{dx_2}{dt} = x_3, \\ \frac{dx_3}{dt} = a_{\psi\delta}(t)x_4 + \bar{M}_z(t), \\ \frac{dx_4}{dt} = x_5, \\ \frac{dx_5}{dt} = x_6, \\ \frac{dx_6}{dt} = (-a_2x_6 - a_3x_5 - x_4 + K_px_2 + K_dx_3)\frac{1}{a_1}, \end{cases}$$

where $a_1 = \tau_1\tau_2^2, a_2 = 2\zeta\tau_1\tau_2 + \tau_2^2$ and $a_3 = \tau_1 + 2\zeta\tau_2$.

Consider the initial values of z, $\dot{z}$ and δ as 0, the initial yaw angle ψ as 2.5^o (0.044 rad) and yaw velocity $\dot{\psi}$ as 0.044 rad/s. By setting the SM damping factor $\zeta = 0.4$, it was found that the angle and velocity of yaw are controllable for $K_p = 1.33$ and $K_d = 0.2$. This result was found for the stability area constructed at $t = 0.6$s, with time constants $\tau_1 = 0.001$s and $\tau_2 = 0.02$s. See Figure 14.

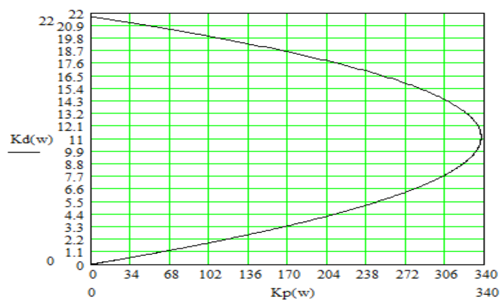

Figure 14. Area of stability

After the study of stability area, the simulation of system with time-varying parameters is represented by polynomials $a_{z\psi}(t), a_{z\delta}(t), a_{\psi\delta}(t)$. The parameters have been set as $\tau_1 = 0.001$, $\tau_2 = 0.02$, $K_p = 1.33$, $K_d = 0.2$ and $\zeta = 0.4$. To choose these gains, a lot of simulations taking into account the stability area have been performed.

By varying the time instants, the time constants and proceeding as in the previous section, an extensive study about the

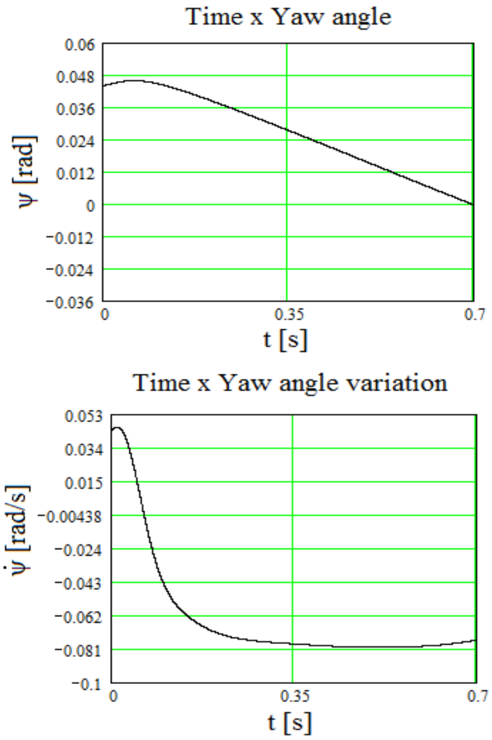

Figure 15. Dynamic system with non-stationary characteristics: yaw and yaw variation versus time

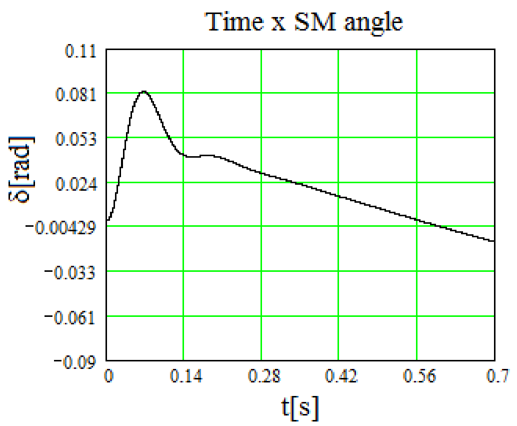

Figure 16. Dynamic system with non-stationary characteristics: SM angle versus time

influences of the parameters in the technical stability area is performed. The study of each one of these areas enables the choice of gains in order to stabilize the system. The goal is to find the value of the parameters leading the initial angle ψ and $\dot{\psi}$ to zero. Control of lateral displacement z and its variation $\dot{z}$ has not been considered in order to simplify the problem.

Figures 15 and 16 shows the obtained values for ψ, $\dot{\psi}$ and δ to validate the control design.

Analyzing Figure 15, it is possible to see that the yaw angle and the variation of yaw approach zero, as expected. These graphics were obtained for an short period of time because the initial values of parameters, before the polynomial regression, are just for 0.7 seconds. Because of that, in the simulation of non-stationary system, the analysis was made for this time interval.

With respect of SM angle δ, it can be seen in Figure 16 that its variation is between 0.081 and -0.015 rad; i.e., it was taken into account the overshoot of δ, $-5^o \leq \delta \leq 5^o$.

7. Conclusions

The stability control problem of third stage rocket using an SM as actuator of a single engine has been addressed. This problem has been approached by obtaining the equations that describe the system, calculating the time-variant model parameters, constructing stability areas, and selecting the structure and parameters of a PD controller.

After choosing the parameters related to the mechanical electro-hydraulic valve structure, and the controller gains, which are applied to the yaw angle and velocity, the problem of obtaining the third stage RC stability inside a technical area could be solved.

The model parameters have direct influence on the stability areas, such as setting of time variant coefficients, which describe the third stage rocket dynamic and actuation system. At every time instant, these coefficients values will generate different stability areas. Studying the stability areas in each instant inside a given interval and the influence of model parameters chosen in these areas, it was possible to find the controller gains to stabilize the yaw angle and velocity, taking care of maximum and minimum values that the engine angle can reach. If the variation angle of engine were greater than the engine overshoot, the time constants of SM should be smaller; i. e., it is necessary an SM with a better valve flow capacity [2].

To illustrate these theoretical results, computational simulations have been presented. However, the problem of controllability maintenance is a challenge and often demands solutions that are not traditional [5]. For future works, it is intended to research and study more about RC as control object and rocket controllability maintenance.

Acknowledgments

The authors want to thank the Brazilian National Council for Technological and Scientific Development (CNPq) and the Brazilian Space Agency (AEB) for the viability of this study.

References

[1] L. Schmid, P. Weiss and B. Johnson, "Hydraulic Servo Control Valve Analysis," WADC Technical Report, pp. 1-45, 1957.

[2] H. E. Merritt, "Electro-Hydraulic Servo Valve Construction, Models and Use," Hydraulic Control Systems, 1967.

[3] Y. D. Sheptun, G. M. Totska, "Calculation of Hydraulic servo using a PC," PBB University, 2002.(in Russian)

[4] M. D. Griffin and J. R. French, J. A. Schetz, Space Vehicle Design. American Institute of Aeronautics and Astronautic, 2004.

[5] I. M. Igdalov, L. D. Kuchma, N. V. Polyakov and Y. D. Sheptun, S. N. Konyukhov, Rocket as a control object. Dniepropetrovsk, Art - Press, 2004. (in Russian)

[6] R. Poley, "DSP Control of Electro-Hydraulic Servo Actuators," SPRAA - Texas Instrument, vol. 76, pp. 1-25, 2005.

[7] F.P. Wijnheijmer, "Modelling and control of a hydraulic servo system H_∞ control and LPV control versus classical control," Master's thesis, University of Technology Eindhoven (TU/e), Department of Mechanical Engineering, Division Dynamical Systems Design, Control System Technology group, 2005.

[8] D. V. Lazic and M. R. Ristanovic, "Electrohydraulic thrust vector control of twin rocket engines with position feedback via angular transducers," Control Engineering Practice, vol. 15, pp. 583-594, 2007.

[9] B. Wie, W. Du and M. Whorton, "Analysis and Design of Launch Vehicle Flight Control Systems," NASA - Launch vehicles and launch operations, pp. 1-11, 2008.

[10] K. M. Elbayomy, J. Zongxia and Z. Huaqing, "PID Controller Optimization by GA and Its Performances on the Electro-hydraulic Servo Control System," Chinese Journal of Aeronautics, vol. 21, pp. 378-384, 2008.

[11] S. Wenhai and J. Jihai, "Adaptive Fuzzy Sliding-Mode Control for Direct Drive Electro-Hydraulic Servo Rocket Rudder," IEEE, vol. 8, 2008.

[12] V. Balasoiu and M. O. Popoviciu, "Model mathematical for hydraulic axes, servovalve electrohydraulic - linear motor," Machine Design, pp. 167-172, 2009.

[13] R. Dolid, PMP, The Electrohydraulic Servovalve Coloring Book. MTS Systems Corporation, 2010.

[14] I. M. Igdalov, L. D. Kuchma, N. V. Polyakov and Y. D. Sheptun, Academician S.n. N. Konyuhovf, The dynamic design of rockets. Dniepropetrovsk Publishers, 2010.(in Russian)

[15] K. Dasgupta and H. Murrenhoff, "Modeling and dynamics of a servo-valve controlled hydraulic motor by bondgraph," Mechanism and Machine Theory - ScienceDirect, vol. 46, pp. 1016-1035, 2011.

[16] I. M. Igdalov, L. D. Kuchma, N. V. Polyakov and Y. D. Sheptun, Dynamic design rockets. Dniepropetrovsk Publishing, 2011.(in Ukrainian)

[17] R. Rodriguez, "Study of a nozzle vector control for a low cost mini-launcher," Master's thesis, University of Catalonia, 2011.

[18] T. A. Kovalenko, N. D. Kovalenko and Y. D. Sheptun, "Comparison of controls mechanism of stage space vehicle," Rocket - Space Technique, vol. 14, pp. 65-71, 2011.(in Russian)

[19] A. Tewari, Thomson Digital, Advanced control of aircraft, spacecraft and rockets. John Wiley and Sons Ltd., 2011.

[20] J. R. Hervas and M. Reyhanoglu, "Thrust Vector Control of an Upper-Stage Rocket with Multiple Propellant Slosh Modes," Hindawi Publishing Corporation Mathematical Problems in Engineering, pp. 2-18, 2012.

[21] Glenn Learning Technologies Project, "Fundamentals of Rocket Stability." Available: `http://www.rockets4schools.org/images/Fundal.Rocket.Stability.pdf`

[22] J. W. Jang, A. Alaniz, R. Hall, N. Bedrossian, C. Hall, and M. Jackson, "Design of Launch Vehicle Flight Control Systems Using Ascent Vehicle Stability Analysis Tool," in Proc. AIAA Guidance, Navigation and Control Conference, 2011.

BIOGRAPHY

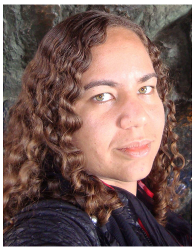

Adriana Elysa Alimadro Corrêa graduated in Physics bachelor from the University of Brasilia, Brazil, in 2010. Participated in design of scientific initiative in 2008 to study the confinement of plasma in magnetic fields and their behavior for their use in rocket thrusters. In 2009 worked as intern in Brazilian Space Agency acting in AEB School Program in aid in the production of scientific outreach events and participated in them as monitors, exhibitor and disseminator of Space Science. In 2011-2012 successfully completed training at Physical-Technical Faculty of Dniepropetrovsk National University Oles Gonchar at Ukraine in aerospace domain, specifically courses under Masters Degree. In 2011-2012 also successfully completed general training courses in aerospace domain at Yuzhnoye State Design Office at Ukraine. Currently, she is concluding a Masters Degree in electronic systems engineering and automation within aerospace at University of Brasilia, Brazil.

Yuri Dmitrievich Sheptun graduated from the University of Kiev in 1958 and chief engineer of office of the group of researchers from research pilot plant design department of engineering manufactures in the Soviet Socialist Republic (city of Votkinsk, 1958-1961) and Yuzhnoye (Dniepropetrovsk, 1961-1965). Professor of DGU in 1966-1983. From 1984 to the present day, chief of robotics department at the Physical-Technical Institute of DNU. PhD in 1965, associate professor in 1967, doctor of technical sciences in 1972 and professor in 1973. Designer of preliminary designs sections for the management and stability of the rocket. Scientific director and performer research on the dynamics of control rocket which took place in Dniepropetrovsk in the implementation of the Soviet government in relation to the scientific support for the project Yuzhnoye. Author of 260 scientific works, including 12 books and 15 inventions. Worked on committees scientific-methodical of Committee of the USSR and Ministry of Education of Ukraine in the two qualifications of advisors specialized in theory, in Research Center for training and professional scientists. Head of the Regional Center of New Information Technologies in DNU, co-author of the concept of comprehensive computer support of the educational process, implemented through the Regional Center for several high schools in the region. Honorary Professor of the DSU (1998). As co-author of the concept of lifelong learning, won the first prize of the Ministry of Education of Ukraine (1992). He was awarded the medal "For value of work" (1982) and the Order "For Merit" grade III (2001). Has published four books.

Alex da Rosa was born in Goiânia-GO, Brazil, in 1980. He received his B.Sc. degree in Electrical Engineering from the Federal University of Goiás (UFG) in 2002, and his M.Sc. and Ph.D. degrees in Electrical Engineering from the School of Electrical and Computer Engineering of the State University of Campinas (UNICAMP) in 2005 and 2009, respectively. He is currently with the Department of Electrical Engineering of the University of Brasília. His research interests include the areas of modeling and identification of nonlinear dynamic systems.

Henrique Cezar Ferreira has a Bachelor degree in Electrical Engineering from the Polytechnic University of São Paulo (2003), where he also obtained a Master (2004) and a Ph.D. (2008) degree in Electrical Engineering. He is currently an associate professor at the University of Brasilia and a control system researcher affiliated with the Laboratory of Automation and Robotics (LARA). He has experience in Engineering Electric, with emphasis on control of electronic process, feedback systems, working mainly in the following topics: robust control robust, nonlinear control, process control, optimization and magnetic levitation.

João Yoshiyuki Ishihara has a Bachelor degree in Electrical Engineering from the Polytechnic University of São Paulo (1990), where he also obtained a Master (1996) and a Ph.D. (1998) degree in Electrical Engineering. From 1998 to 2002 he held a post-doctoral position at the Engineering School of São Carlos, University of São Paulo. Since 2004 is an assistant professor at the University of Brasilia and a control system researcher affiliated with the Laboratory of Automation and Robotics (LARA). He has experience in Electrical Engineering with emphasis on control of electronic process, feedback systems, working mainly in the following topics: robust control and filtering, descriptor systems, systems with Markovian jumps. João Ishihara is a Fellow Researcher of Productivity of the National Council for Scientific and Technological Development (CNPq).

Renato Alves Borges received a Master (2004) and a Doctoral (2009) degree in Electrical Engineering from the University of Campinas and a PhD degree in Electrical Engineering from the University of New Mexico (2009) (USA). From 2009 to 2011 he held a post-doctoral fellowship from the State of São Paulo Research Foundation working at the School of Electrical and Computer Engineering at the University of Campinas. He is currently an assistant professor at the Electrical Engineering Department of the University of Brasilia, and a control system researcher affiliated with the Laboratory of Automation and Robotics (LARA). His main research interests are Lyapunov stability theory, stability analysis of uncertain linear and nonlinear systems, and linear systems with parameter variations and finite-time stability.